

Critical behaviour in the elastic response of hydrogels

M. Dennison^{1,3}, M. Jaspers², P.H.J. Kouwer², C. Storm³, A.E. Rowan², and F.C. MacKintosh¹

¹*Department of Physics and Astronomy, VU University,
De Boelelaan 1081, 1081 HV Amsterdam, The Netherlands*

²*Radboud University Nijmegen, Institute for Molecules and Materials,
Department of Molecular Materials, Heyendaalseweg 135, 6525 AJ Nijmegen, The Netherlands and*

³*Department of Applied Physics and Institute for Complex Molecular Systems,
Eindhoven University of Technology, P.O. Box 513, 5600 MB Eindhoven, The Netherlands*

(Dated: December 6, 2024)

Highly responsive, or ‘smart’ materials are abundant in Nature; individual cells, for instance, can adapt their mechanical properties to the local surroundings through small changes in their internal structure. An effective method to enhance the responsiveness of *synthetic* materials is to operate near a critical point, where small variations lead to large changes in material properties. Recent theories have suggested that fibre/polymer networks can show critical behaviour near and below the point of marginal connectivity that separates rigid and floppy states [1–4]. To date, however, experimental evidence for criticality in such networks has been lacking. Here, we demonstrate critical behaviour in the stress response of synthetic hydrogels at low concentrations of order 0.1% volume fraction. We show, using computer simulations, that the observed response to stress can be understood by considering the influence of a zero-temperature critical point, i.e. the Maxwell isostatic point [5], together with the intrinsically nonlinear stretch response of semi-flexible polymer strands in the gel.

The isostatic point identified 150 years ago by Maxwell [5] has proven to be a rich source of inspiration for novel physics, ranging from jamming [6, 7] to zero-temperature critical behaviour [1, 2] and even non-quantum topological matter [8]. However, most of this work has been theoretical, and experimental realisations of such criticality have been limited to granular and colloidal particle packings, which exhibit a critical point at the jamming transition. At this point, various signatures of criticality can be seen, including a shear modulus that varies with the volume fraction ϕ as $G \sim |\phi - \phi_c|^{1/2}$ [6, 7], where ϕ_c is the jamming point which is of order unity. Interestingly, fibre networks are expected to show similar critical behaviour at much lower concentrations than jammed particle packings.

There remain important experimental challenges, however, in creating networks near a critical point, including controlling microstructural parameters. Network connectivity z is a particularly important parameter, since it quantifies the distance from the isostatic point z_c at which the number of degrees of freedom is just balanced by the number of constraints imposed by connecting polymer strands: networks are rigid for higher connectiv-

ities and floppy below this point. The synthetic hydrogels we study have recently been shown to allow a high degree of control over both the network connectivity and the filament properties [9]. Above their gel point, these hydrogels exhibit a nonlinear elastic response similar to many biopolymer systems, in which the network stiffness, defined by the differential shear modulus $K = d\sigma/d\gamma$, increases with increasing shear strain γ , and scales with shear stress σ as $\sigma^{3/2}$ [10, 11]. Here, we focus on the regime near and below the gel point, where we find a *sub-linear* stiffening response to an applied shear strain, with $K \propto \sigma^{\alpha < 1}$, and we show that this unexpected nonlinear elastic response is a consequence of criticality associated with the isostatic critical point. Importantly, this work implies that the influence of isostaticity can extend to network connectivities very far below the isostatic critical point.

We performed rheology experiments in both linear and nonlinear elastic regimes for a range of temperatures near the gel point for this system. For temperatures in the range from 19.5 to 21° C, we observe a weak initial linear elastic regime, followed by a power-law stiffening with $K \propto \sigma^\alpha$ and $\alpha \simeq 0.64$ (see inset to Fig. 1). The linear shear modulus G_0 appears to vanish for temperatures below $T \simeq 19^\circ$ C, which we identify as the gel point for our system. For lower temperatures, in the range of 17 to 19° C, we observe an initial nonlinear regime with $\alpha \simeq 0.8$ over about an order of magnitude in stress, as shown in Fig. 1.

The observed stiffening exponents $\alpha \simeq 0.64$ and $\alpha \simeq 0.8$ are consistent with recently predicted nonlinear elasticity of spring networks near and below the isostatic, or *marginal*, point [1, 3]. Near the marginal point in spring networks, a variety of critical behaviours are predicted, including an approximate square-root dependence on various stabilizing fields, such as stress [1, 3], thermal fluctuations [4] and bending rigidity [2]. A simple mean-field argument suggests the appearance of $K \sim \sigma^\alpha$ with $\alpha \simeq 1/2$: in a marginal network, the linear shear modulus vanishes but any finite stress stabilises the network, such that the modulus increases with strain γ as $|\gamma|$, resulting in $\sigma \sim \gamma^2$ and $d\sigma/d\gamma \sim \sigma^{1/2}$ [1, 12].

Thus, an approximate square-root dependence of K on stress is expected near the critical, or marginal, state, indicated by the $\alpha \simeq 1/2$ regime in the phase diagram in Fig. 2. Below this marginal state, in a regime of ini-

tially floppy systems, an approximate linear dependence of K on the stabilising field σ is expected, much as a linear dependence of the magnetisation is expected in a paramagnetic-like phase. Importantly, however, the *critical* regime indicated by $\alpha \simeq 1/2$ is not limited to systems finely-tuned to the naïve isostatic connectivity, z_c , but, depending on the applied stress, is expected to persist to much lower connectivities [2–4]. Our simulations demonstrate this, as well as showing exponents α that deviate from the mean-field values. Moreover, as the stress is increased beyond the initial $K \sim \sigma^\alpha$ regime, our gels exhibit a second stiffening regime, for which we define a second exponent $\beta \simeq 1.2$ that is distinct from the asymptotic exponent of 1.5 observed previously [9]. We hypothesise that this arises from the nonlinear effective spring constant of the polymers making up the network [9–11, 13, 14]. As the stress increases, these polymers stretch and enter a nonlinear regime characterised by a force-extension relation in which the force $f \sim 1/|1 - \epsilon|^2$ [13, 15, 16] depends on the extension ϵ relative to full extension ($\epsilon = 1$). An effective spring constant $k_{\text{sp}} \propto f^{3/2}$ emerges, where $f \propto \sigma$ is the force on the polymer. This results in a stress dependence given by [3] $K \sim \sigma^\alpha \times k_{\text{sp}}^{1-\alpha} \sim \sigma^\beta$, where

$$\beta = 3/2 - \alpha/2. \quad (1)$$

In order to test this, we perform computer simulations on 2D and 3D networks consisting of model polymers connected at N nodes, with the nodes acting as cross-links between filament segments. The systems contain $N_f = zN/2$ segments where z is the average coordina-

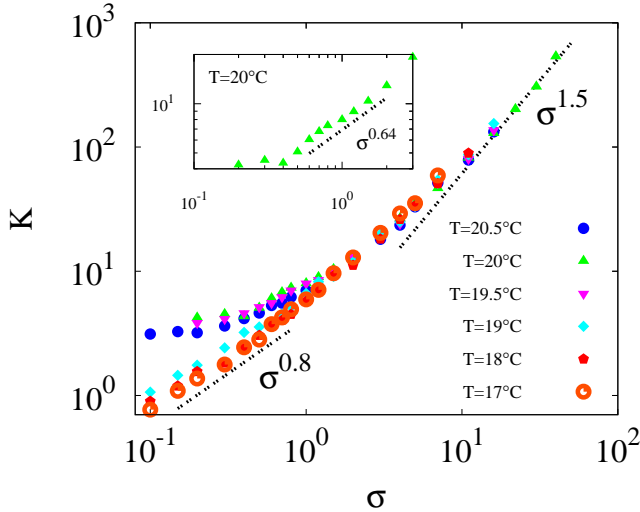


FIG. 1. **Experimental differential shear modulus** Differential shear modulus $K = \partial\sigma/\partial\gamma$, where γ is the shear strain, against shear stress σ for hydrogels from temperature $T = 17^\circ\text{C}$ to 20.5°C . The lines indicate power-law dependencies of K vs σ . The inset shows the same data, focusing on the initial sublinear scaling regimes for $T = 20^\circ\text{C}$. All axes are in units of Pa.

tion number (connectivity) of the network. We consider network topologies where the nodes are arranged on a lattice. The connectivity is lowered by removing randomly chosen segments, and the networks become mechanically floppy below a critical connectivity $z_c \simeq 2d$, where d is the dimensionality [2, 5]. We use two types of model filaments (see methods), the first of which is a chain of Hookean springs. Here, in contrast to real semi-flexible polymers, the filament segments may stretch indefinitely and they show only a linear force vs extension, which is not expected to accurately describe our experimental system at high stress, but can describe the behaviour at low stress. In order to capture the behaviour of semi-flexible polymers, we use a second model where the filament stretch response is initially linear, followed by a strong stiffening due to the pulling out of thermal bending modes. In both models, the filament stiffness is controlled by an effective spring constant k_{sp} , which is related to the ratio of the persistence length to the segment contour length ℓ_p/ℓ_0 (see supplemental material [17]).

We first show the behaviour of the modulus K as a function of σ for simulated 2D and 3D networks us-

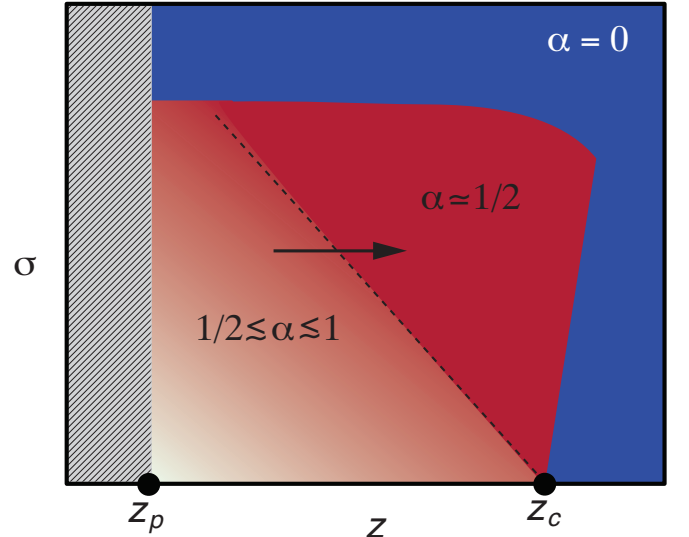


FIG. 2. **Phase diagram** Schematic phase diagram of the various regimes of network response as a function of connectivity z (average coordination of network nodes) and stress σ . Here, z_c is the critical connectivity, above which a purely Hookean network becomes mechanically rigid at zero temperature and stress, while z_p is the percolation point. The exponent α indicates different regimes of stress dependence, characterised by network stiffness $K \sim \sigma^\alpha k_{\text{sp}}^{1-\alpha}$, where k_{sp} is the spring constant. The critical regime, governed by the isostatic point, where α is approximately given by the mean-field value of $1/2$, is indicated in red. In the lower left ($1/2 \lesssim \alpha \lesssim 1$) regime, α gradually increases toward 1 as z is decreased. The arrow indicates the direction taken as we increase the temperature in our experimental hydrogels.

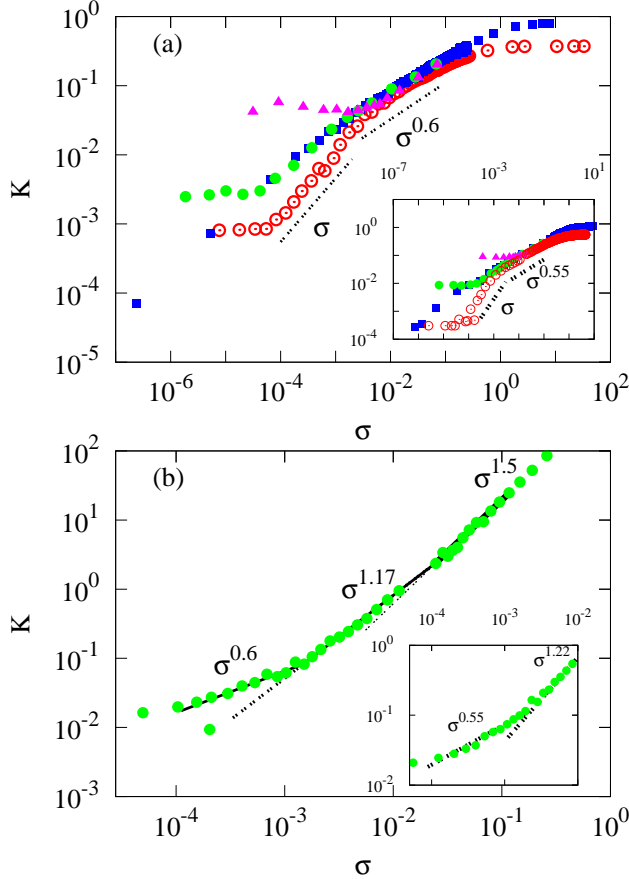


FIG. 3. **Simulation differential modulus** Top: Differential shear modulus K vs stress σ for (main plot) 2D lattice networks with $z = 3.85 \lesssim z_c \simeq 3.857$ (solid symbols) and $z = 3$ (open symbols), and (inset) 3D lattice networks with $z = 5.84 \lesssim z_c \simeq 5.844$ (solid symbols) and $z = 4$ (open symbols) using Hookean springs. For 2D networks, K and σ are in units of the spring constant k_{sp} , while for 3D networks the units are k_{sp}/ℓ_0 where ℓ_0 is the rest length of the springs (which also gives the segment contour length). Squares show $\ell_p/\ell_0 = \infty$ (no thermal fluctuations), circles $\ell_p/\ell_0 = 10$ and triangles $\ell_p/\ell_0 = 1$ where ℓ_p is the persistence length of the filaments. Dashed lines show $K \sim \sigma^\alpha$ dependencies. Bottom: K as a function of σ for (main plot) 2D marginal network with connectivity $z = 3.84$, and (inset) 3D marginal network with connectivity $z = 5.84$, using semi-flexible filaments (see methods), with $\ell_p/\ell_0 = 10$. Both axes are in units of k_{sp} for 2D networks, while for 3D networks the units are k_{sp}/ℓ_0 , where here k_{sp} is an effective spring constant [17]

ing Hookean springs. For systems close to the marginal point (Fig. 3(a)), we find that athermal networks, where $\ell_p/\ell_0 \rightarrow \infty$ [17], exhibit no initial linear response to an applied shear strain γ . As the temperature is increased, ℓ_p/ℓ_0 decreases, and a linear response regime emerges where we find $K = G_0$. This initial linear shear modulus is known to have a mixed dependency, with both the spring constant and thermal fluctuations [4] contributing, and it increases (in units of k_{sp}) as ℓ_p/ℓ_0 decreases.

This is followed by an increase in K once the stress exceeds a critical value σ_c , giving a $K \sim \sigma^\alpha$ dependence with $\alpha < 1$. For 2D networks we find $\alpha \sim 0.6$ while for 3D networks we see $\alpha \sim 0.55$, which are similar to the values observed experimentally and also close to the mean-field value of $\alpha = 1/2$ [1]. As the modulus and stress have the same units, on dimensional grounds, K should then show an additional dependence on the other energy scales in our model, i.e., either the spring constant or the temperature. Finally, at high stresses, we see that K becomes invariant to σ and begins to scale as $K \sim k_{sp}$, corresponding to pure stretching of the springs. We note that the size of the $K \sim \sigma^\alpha$ stiffening regime is sensitive to the ratio ℓ_p/ℓ_0 ; if this ratio is too small, G_0 will be large enough to dominate the response.

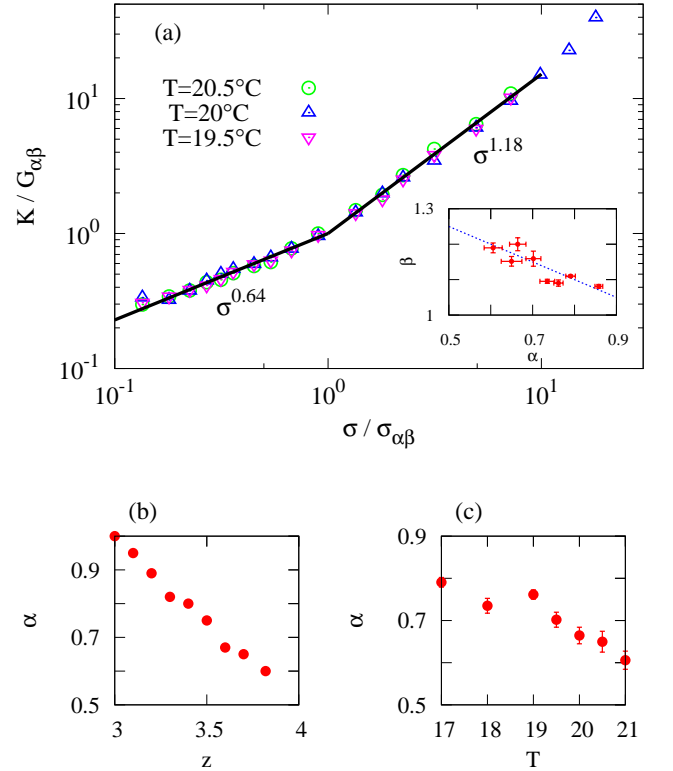


FIG. 4. **Critical behaviour** (a) Differential shear modulus K against stress σ for experimental systems at $T = 19.5$ to 20.5° C. K is normalized by the shear modulus $G_{\alpha\beta}$ at the cross-over from the α to β regimes and σ is normalized by the corresponding stress. Solid lines show $K \sim \sigma^{0.64}$ and $K \sim \sigma^{1.18}$ dependence. Inset: values of α and β found for individual temperatures ranging from $T = 17$ to 21° C. Line shows the relation $\beta = 1.5 - 0.5\alpha$. (b) Initial stiffening exponent α against connectivity z for simulated 2d Hookean spring networks, showing an evolution in α from $\sim 1/2$ towards ~ 1 as z is lowered. A qualitatively similar trend is also found for semi-flexible networks and also for 3d networks. (c) α against T for experimental networks.

For networks below the marginal point we find, after the initial linear response G_0 regime, a stress dependent

regime with a stiffening exponent α that increases as z decreases. This eventually shows an approximate linear stress dependence, where $K \sim \sigma$, at sufficiently low z , as can be seen in Fig. 3(a). Interestingly, we find that as we increase the stress, even sub-marginal networks can exhibit marginal behaviour with $\alpha \simeq 1/2$. Thus, the influence of the isostatic point extends well below $z = z_c$. Finally, we again find a pure k_{sp} dependence at high stress.

In order to understand the intermediate regime corresponding to $1\text{Pa} \lesssim \sigma \lesssim 10\text{Pa}$ in Fig. 1, which was not observed in our simulations with Hookean springs, we simulated networks with the nonlinear response of semi-flexible filaments incorporated. Our results are shown for both 2D and 3D networks in Fig. 3(b). Following an initial $K \sim \sigma^\alpha$ stiffening, where α has the same value as for Hookean spring networks, we find both $K \sim \sigma^\beta$ and $K \sim \sigma^{3/2}$ regimes, where β obeys Eq. (1). This is in agreement with the phase diagram in Fig. 2, with both $K \sim \sigma^\alpha \times k_{\text{sp}}^{1-\alpha}$ at intermediate stress and $K \sim k_{\text{sp}}$ at high stress, where $k_{\text{sp}} \propto \sigma^{3/2}$, consistent with known extensional properties of semi-flexible polymers [9–16]. These observations can account for our experimental results for $1\text{Pa} \lesssim \sigma \lesssim 10\text{Pa}$. In Fig. 4, we show data for experimental networks at $T = 19.5 - 20.5^\circ\text{C}$ with K (and σ) scaled by the shear modulus $G_{\alpha\beta}$ (and stress $\sigma_{\alpha\beta}$) at which we observe the cross-over from α to β regimes. Here we find an excellent collapse of the data with $\alpha \sim 0.64$ and $\beta \sim 1.18$. In the inset we show the values of α and β found for temperatures from 17 to 21°C , which again show good agreement with the relation given in Eq. (1). Importantly, the prediction (dashed line) contains no adjustable parameters. Finally, we also observe an evolution of the exponent α as the temperature is decreased (Fig. 4(c)). This is consistent with the trend predicted in the simulations where the initial stiffening exponent α increases from approximately $1/2$ near the marginal point towards $\alpha \simeq 1$ as one moves to lower z values (Fig. 4(b)). This behaviour is indicated in the schematic phase diagram in Fig. 2 by the solid arrow, corresponding to the exponent one would find for increasingly large temperatures at a given stress.

These results show that synthetic hydrogels exhibit an elastic response consistent with predicted critical behaviour associated with isostatic and sub-isostatic networks. Surprisingly, even networks deep into the sub-isostatic regime are able to exhibit such behaviour. This suggests that the marginal point is an important mechanism for controlling the elastic response of networks, and our results support the phase diagram in Fig. 2, indicating a very broad range over which critical control of network mechanics is possible. We also identify the ratio of the persistence length to the cross-link separation, ℓ_p/ℓ_0 , as a key design parameter, which should be of the order of $0.1 - 10$ to achieve critical control of network mechanics. When the polymers are too flexible, for instance, the linear shear modulus dominates over the critical stiffening behaviour. Thus, for synthetic poly-

mers that are usually flexible, controlled bundle formation may be important for future materials development using these principles. In summary, this work demonstrates an experimentally realizable system that exhibits mechanical critical behaviour, opening the way for further experimental studies of marginal/isostatic networks.

METHODS

Experiment. Our gels were synthesised and purified following a previously described procedure [9]. The catalyst/monomer ratio of $1 : 2000$ yielded a polymer of average molecular weight $M_v = 400\text{ kg mol}^{-1}$ as determined by viscometry. For gel studies, the polymer was dissolved in purified water (milliQ) by stirring for at least 24 hrs at 4°C . Rheology was performed with a stress-controlled rheometer (Discovery HR-1, TA Instruments) with an aluminium parallel plate geometry (40 mm diameter) and a gap of $500\text{ }\mu\text{m}$. Samples were inserted in the rheometer at 5°C (i.e. as a liquid) and gelation occurred between the parallel plates by raising the temperature. Drying of the sample was prevented by maintaining a moist atmosphere. The storage modulus in the linear regime was obtained by applying an oscillatory strain of 1% at a frequency of 1 Hz and measuring the sinusoidal stress response. The non-linear regime was probed by applying a steady pre-stress σ to the sample and superposing a small oscillatory stress with an amplitude of $|\delta\sigma| < 0.1\sigma$ at a frequency of $0.1 - 10\text{ Hz}$. The differential modulus was calculated from the oscillatory strain response $\delta\gamma$, as $K = \partial\sigma/\partial\gamma = \delta\sigma/\delta\gamma$.

Simulation. Our simulations use lattice based networks, where the network nodes are arranged on a triangular lattice in 2D and on an FCC lattice in 3D. Nearest neighbour nodes are then linked with filament segments to give fully connected networks with $z = 6$ in 2D and $z = 12$ in 3D. We initially consider Hookean springs as the model segments, which have been used in many previous studies [2–4, 18] and for which stretching and compression of a segment i involves an energy cost given by

$$\mathcal{U}_s = \frac{k_{\text{sp}}}{2}(\ell_i - \ell_{0,i})^2, \quad (2)$$

where ℓ_i is the length and $\ell_{0,i}$ is the contour length of segment i . We also use a potential which more accurately describes the experimental filaments [19]. The full model is outlined in the supplemental material [17], and can be summarized by the force along a stretched segment which is given by

$$f = \frac{9k_{\text{B}}T\ell_p}{\ell_{0,i}^2} \left[\frac{1}{(1-\epsilon)^2} - 1 - \frac{1}{3}\epsilon \right], \quad (3)$$

where the dimensionless extension $\epsilon = 6\ell_p(\ell_i - \ell_{0,i})/\ell_{0,i}^2$. This force diverges near full extension, where $\epsilon \rightarrow 1$.

Here, T is the temperature, k_B the Boltzmann constant and ℓ_p is the persistence length of the filaments. For lattice networks, the contour lengths are identical for all segments. We note that for the results presented here we do not apply a bending stiffness to the filaments for reasons of computational efficiency, as it can be shown that this does not effect the stiffening behaviour we observe [17]. We use Lees-Edwards boundary conditions to shear networks [20] with periodic boundary conditions. After applying a shear strain γ to the system, we calculate the shear stress σ and differential modulus K as described in Refs. [4, 21].

ACKNOWLEDGMENTS

We acknowledge financial support from FOM/NWO (M.D, C.S, F.C.M), NRSCC (M.J, A.E.R) NWO Gravitation (A.E.R, P.H.J.K) and NanoNextNL (A.E.R, P.H.J.K). We would like to thank David Weitz for fruitful discussions and suggestions.

M.D, C.S and F.C.M designed the simulations. M.D. performed the simulations. M.J, P.H.J.K and A.E.R designed the experimental work. M.J. synthesised the polymers and carried out the mechanical tests. All authors contributed to the writing of the paper.

-
- [1] M. Wyart, H. Liang, A. Kabla, and L. Mahadevan, *Phys. Rev. Lett.* **101**, 215501 (2008).
 - [2] C. P. Broedersz, T. C. Lubensky, X. Mao, and F. C. MacKintosh, *Nature Physics* **7**, 983 (2011).
 - [3] M. Sheinman, C. P. Broedersz, and F. C. MacKintosh, *Phys. Rev. Lett.* **109**, 238101 (2012).
 - [4] M. Dennison, M. Sheinman, C. Storm, and F. C. MacKintosh, *Phys. Rev. Lett.* **111**, 095503 (2013).
 - [5] J. C. Maxwell, *Philos. Mag.* **27**, 297 (1864).
 - [6] A. J. Liu and S. R. Nagel, *Annu. Rev. Condens. Matter Phys.* **1**, 347 (2010).
 - [7] M. van Hecke, *J. Phys.: Condens. Matter* **22**, 033101 (2010).
 - [8] C. L. Kane and T. C. Lubensky, *Nature Physics* **10**, 39 (2013).
 - [9] P. H. J. Kouwer, M. Koepf, V. A. A. Le Sage, M. Jaspers, A. M. van Buul, Z. H. Eksteen-Akeroyd, T. Woltinge, E. Schwartz, H. J. Kitto, R. Hoogenboom, S. J. Picken, R. J. M. Nolte, E. Mendes, and A. E. Rowan, *Nature* **493**, 651 (2013).
 - [10] M. L. Gardel, J. H. Shin, F. C. MacKintosh, L. Mahadevan, P. Matsudaira, and D. A. Weitz, *Science* **304**, 1301 (2004).
 - [11] Y. C. Lin, N. Y. Yao, C. P. Broedersz, H. Herrmann, F. C. MacKintosh, and D. A. Weitz, *Phys. Rev. Lett.* **104**, 058101 (2010).
 - [12] C. P. Broedersz and F. C. MacKintosh, *arXiv:1404.4332* (2014).
 - [13] F. C. MacKintosh, J. Kas, and P. Janmey, *Phys. Rev. Lett.* **75**, 4425 (1995).
 - [14] C. Storm, J. J. Pastore, F. C. MacKintosh, T. C. Lubensky, and P. A. Janmey, *Nature* **435**, 191 (2005).
 - [15] M. Fixman and J. Kovac, *The Journal of Chemical Physics* **58**, 1564 (1973).
 - [16] J. F. Marko and E. D. Siggia, *Macromolecules* **28**, 8759 (1995).
 - [17] See Supplemental Material at [URL will be inserted by publisher].
 - [18] C. P. Broedersz, M. Sheinman, and F. C. MacKintosh, *Phys. Rev. Lett.* **108**, 078102 (2012).
 - [19] A. M. van Buul, E. Schwartz, P. Brocorens, M. Koepf, D. Beljonne, J. C. Maan, P. C. M. Christianen, P. H. J. Kouwer, R. J. M. Nolte, H. Engelkamp, K. Blank, and A. E. Rowan, *Chemical Science* **4**, 2357 (2013).
 - [20] A. W. Lees and S. F. Edwards, *J. Phys. C* **5**, 1921 (1972).
 - [21] D. R. Squire, A. C. Holt, and W. G. Hoover, *Physica* **42**, 388 (1969).